Evidence for Abiotic Dimethyl Sulfide in Cometary Matter

Hänni, Nora; Altwegg, Kathrin; Combi, Michael; Fuselier, Stephen A.; De Keyser, Johan; Ligterink, Niels F.W.; Rubin, Martin; Wampfler, Susanne F.

DOI
10.3847/1538-4357/ad8565

Publication date
2024

Document Version
Final published version

Published in
Astrophysical Journal

The Astrophysical Journal, 976:74 (8pp), 2024 November 20 https://doi.org/10.3847/1538-4357/ad8565

Evidence for Abiotic Dimethyl Sulfide in Cometary Matter

Nora Hänni[1], Kathrin Altwegg[1], Michael Combi[2], Stephen A. Fuselier[3,4], Johan De Keyser[5], Niels F. W. Ligterink[1,6], Martin Rubin[1], and Susanne F. Wampfler[7]
[1] Physics Institute, Space Research & Planetary Sciences, University of Bern, Sidlerstrasse 5, CH-3012 Bern, Switzerland; nora.haenni@unibe.ch
[2] Department of Climate and Space Sciences and Engineering, University of Michigan, Ann Arbor, MI, USA
[3] Space Science Division, Southwest Research Institute, San Antonio, TX, USA
[4] Department of Physics and Astronomy, The University of Texas at San Antonio, San Antonio, TX, USA
[5] Royal Belgian Institute for Space Aeronomy, BIRA-IASB, Brussels, Belgium
[6] Faculty of Aerospace Engineering, Delft University of Technology, Delft, The Netherlands
[7] Center for Space and Habitability, University of Bern, Gesellschaftsstrasse 6, CH-3012 Bern, Switzerland
Received 2024 April 25; revised 2024 October 5; accepted 2024 October 8; published 2024 November 14

Abstract

Technological progress related to astronomical observatories such as the recently launched James Webb Space Telescope (JWST) allows searching for signs of life beyond our solar system, namely, in the form of unambiguous biosignature gases in exoplanetary atmospheres. The tentative assignment of a 1σ–2.4σ spectral feature observed with JWST in the atmosphere of exoplanet K2-18b to the biosignature gas dimethyl sulfide (DMS; sum formula C_2H_6S) raised hopes that, although controversial, a second genesis had been found. Terrestrial atmospheric DMS is exclusively stemming from marine biological activity, and no natural abiotic source has been identified—neither on Earth nor in space. Therefore, DMS is considered a robust biosignature. Since comets possess a pristine inventory of complex organic molecules of abiotic origin, we have searched high-resolution mass spectra collected at comet 67P/Churyumov–Gerasimenko, target of the European Space Agency's Rosetta mission, for the signatures of DMS. Previous work reported the presence of a C_2H_6S signal when the comet was near its equinox, but distinction of DMS from its structural isomer ethanethiol remained elusive. Here we reassess these and evaluate additional data. Based on differences in the electron ionization-induced fragmentation pattern of the two isomers, we show that DMS is significantly better compatible with the observations. Deviations between expected and observed signal intensities for DMS are $<1\sigma$, while for ethanethiol they are 2σ–4σ. The local abundance of DMS relative to methanol deduced from these data is $(0.13 \pm 0.04)\%$. Our results provide the first evidence for the existence of an abiotic synthetic pathway to DMS in pristine cometary matter and hence motivate more detailed studies of the sulfur chemistry in such matter and its analogs. Future studies need to investigate whether or not the present inference of cometary DMS could provide an abiotic source of DMS in a planetary atmosphere.

Unified Astronomy Thesaurus concepts: Comet volatiles (2162); Biosignatures (2018); Mass spectrometry (2094)

1. Introduction

Based on data collected during an Earth flyby by the NASA spacecraft Galileo, C. Sagan et al. (1993) proposed that unique molecular indicators of carbon-based life on Earth could be used to search for and detect extraterrestrial life. Today, those indicators are often referred to as biosignatures or sometimes as biomarkers, the latter term being borrowed from the field of medicine. The use of biosignature gases is especially interesting for the search for life in environments like exoplanets that are not accessible by space missions for in situ studies. Currently, potential life on exoplanets is only detectable with remote sensing spectroscopic techniques using ground- or space-based observatories. A recent example is NASA's James Webb Space Telescope (JWST), capable of investigating exoplanetary atmospheres in the near-to-mid-infrared spectral range in unprecedented detail. Taking advantage of the constantly increasing resolving power, wavelength coverage, and sensitivity of exoplanet observatories, S. Seager et al. (2016) compiled a list of terrestrial atmospheric molecules that are produced by biological activity and hence could be employed as biosignatures. Crucial properties of such biosignature gases are, besides volatility, abundance, and stability under exoplanet-like conditions, unique spectral features and the absence of false positives. Beyond the candidates already suggested by C. Sagan et al. (1993), molecular oxygen (O_2; produced by photosynthesis) and methane (CH_4; produced by biology, for example, through methanogenesis), the list in S. Seager et al. (2016) also mentions the simple sulfur-bearing molecule dimethyl sulfide (DMS; C_2H_6S). Methane can be produced by both biotic and abiotic chemical processes, including methanogenic bacteria (R.-S. Taubner et al. 2018) and oceanic hydrothermal vents (J. Horita & M. E. Berndt 1999). This may be relevant, for instance, for Saturn's icy moon Enceladus (A. Bouquet et al. 2015; J. H. Waite et al. 2017). So far, for DMS, no false positives are known. However, F. Raulin & G. Toupance (1975) have shown experimentally that electrical discharge in a gaseous mixture of hydrogen sulfide (H_2S) and methane can lead to the abiotic formation of DMS. DMS falls into the class of low-abundance but unique biosignatures that originate from secondary reactions, i.e., reactions that are not related to energy production or biomass buildup (S. Seager et al. 2016). On Earth, the most relevant and best-studied source of DMS is the degradation of dimethylsulfoniopropionate (DMSP; $C_5H_{10}O_2S$), a sulfur-bearing compound produced by eukaryotic marine phytoplankton and a few higher plants (M. O. Andreae & H. Raemdonck 1983; C. B. Pilcher 2003). DMS, among a handful of small molecules, has been discussed as a potentially

observable indicator of aquatic life on habitable exoplanets with a hydrogen-dominated atmosphere (S. D. Domagal-Goldman et al. 2011; S. Seager et al. 2013; D. C. Catling et al. 2018; E. W. Schwieterman et al. 2018) and, more recently, on a specific class of ocean-covered exoplanets with a hydrogen-rich atmosphere, referred to as Hycean worlds (N. Madhusudhan et al. 2021; F. E. Rigby & N. Madhusudhan 2024). Shortly after, N. Madhusudhan et al. (2023) reported the tentative detection of DMS in the atmosphere of exoplanet K2-18b, a candidate Hycean world, with the JWST using transit spectroscopy. Despite the DMS detection's confidence being only $2.4\sigma/\approx 1\sigma/$ none (depending on how the relative detector offset was accounted for), this work received worldwide attention as it featured DMS as a potential indicator of marine biological activity on this planet, adding though that more conclusive observational constraints on the DMS atmospheric abundance are needed. Better constrained abundances of atmospheric species could also underpin the classification of K2-18b as a Hycean world, which is being debated (C. R. Glein 2024; O. Shorttle et al. 2024; N. F. Wogan et al. 2024). Generally, the search for extraterrestrial life should rely on multiple lines of evidence, see, e.g., D. C. Catling et al. (2018) or E. W. Schwieterman et al. (2018).

We take a different path in this debate by asking if DMS is present in abiotic cometary matter. Comets are known to be rich in refractory and volatile organic matter (S. A. Sandford 2008; A. Bardyn et al. 2017; K. Altwegg et al. 2019) that is thought to be well preserved since the earliest times of our solar system (D. Bockelée-Morvan et al. 2000; M. N. Drozdovskaya et al. 2019; Á. López-Gallifa et al. 2024) and, hence, are a relevant point of reference when it comes to abiotic chemical complexity and diversity.

For this work, we revisited the organosulfur inventory of comet 67P (U. Calmonte et al. 2016; A. Mahjoub et al. 2023) and searched for evidence of the presence of DMS and, hence, for an abiotic source of this molecule. Comet 67P was the target of the European Space Agency's (ESA's) Rosetta mission. It was the first comet to be studied from up close for an extended time period of 2 yr as it passed through perihelion. The Rosetta Orbiter Instrument for Ion and Neutral Analysis (ROSINA; H. Balsiger et al. 2007) with its high-resolution Double Focusing Mass Spectrometer (DFMS) was collecting unique data that unveiled this comet's chemical inventory in unprecedented detail (K. Altwegg et al. 2019; M. Rubin et al. 2019). Many surprising chemical species were detected, from molecular oxygen (A. Bieler et al. 2015) to ammonium salts (N. Hänni et al. 2019; K. Altwegg et al. 2020, 2022; O. Poch et al. 2020) and including a plethora of complex organic molecules (M. Schuhmann et al. 2019a, 2019b; N. Hänni et al. 2022, 2023). U. Calmonte et al. (2016) mentioned the presence of a signal at the exact mass of C_2H_6S in multiple ROSINA/DFMS mass spectra. However, due to overlap with the nearby C_5H_2 signal as well as structural isomerism of DMS (CH_3–S–CH_3) and ethanethiol (CH_3–CH_2–SH), these authors did not make conclusive statements regarding the presence or absence of DMS in comet 67P. Here, we revisit data from U. Calmonte et al. (2016), and thanks to a more precisely constrained mass scale, we arrive at a spectral deconvolution that allows the distinction of DMS and ethanethiol. Technical and methodological details are described in Section 2, while Section 3 presents and discusses our results. Section 4 summarizes our findings, stating how they motivate further research on the sulfur chemistry in the early solar system, and discusses potential implications for exoplanetary science.

2. Instrument and Method

ROSINA/DFMS data collection and reduction have been described in detail by L. Le Roy et al. (2015) and U. Calmonte et al. (2016). In the following, we will therefore limit ourselves to the presentation of the most relevant aspects.

2.1. Data Acquisition with DFMS

DFMS, together with a time-of-flight mass spectrometer and a pressure gauge making up the ROSINA instrument suite (H. Balsiger et al. 2007), was designed to study the volatile species in comet 67P's coma. Cometary neutrals entering the DFMS ionization chamber were subjected to electron ionization (EI) using a 45 eV electron beam. Ions were subsequently extracted from the ion source and passed through an electrostatic analyzer and a permanent magnet, where the electric and magnetic fields led to separation of the species according to their mass-per-charge ratio (m/z). The ions were detected by a stack of two microchannel plates mounted in a Chevron configuration. The released charge was collected on two rows of position-sensitive linear electron detector array anodes. Scanning through the DFMS's mass range was done by stepping from integer mass per charge to integer mass per charge sequentially and took approximately 30 s per mass spectrum, of which 20 s was the integration time. We note that the microchannel plate detector works in analog mode. This means that the charge deposited on the anodes during integration, i.e., the detector signal, depends not only on the number of impacting ions but also on their energy, their structure and size, as well as on the detector gain. The detector gain is determined by the set gain step (i.e., the voltage used to amplify the detector signal) and the individual pixel gain. The latter factor relates to the inhomogeneous detector aging that affects the detector on timescales on the order of weeks and months. The pixel gain is corrected by frequently measured correction factors. Detailed information on pixel gain corrections has been presented in L. Le Roy et al. (2015) and J. De Keyser et al. (2019) or in U. M. Calmonte (2015) and I. R. H. G. Schroeder (2020). In Section 2.3, we estimate the errors, including uncertainties introduced by the detector gain.

The main data set analyzed for this work was collected on 2016 March 15 between 03:30 and 04:14 UTC, during comet 67P's outbound equinox, and covers the mass range $m/z = 13$–100. That day, the most intense C_2H_6S signal was observed, based on the DFMS data evaluated so far. DFMS achieved a mass resolution of $m/\Delta m = 3000$ at 1% of the peak height at $m/z = 28$ (H. Balsiger et al. 2007), which is exceptional for space instruments and allows searching for the fingerprints of specific molecules in a complex analyte mixture, as we explain in detail in the following two subsections.

2.2. EI-induced Fragmentation

EI mostly yields singly charged cations of the analyte molecules, which we refer to as molecular ions (M), or fragments thereof. Fragmentation accompanying the EI process produces the so-called fragmentation pattern of an analyte species, which is the characteristic fingerprint of signals of all

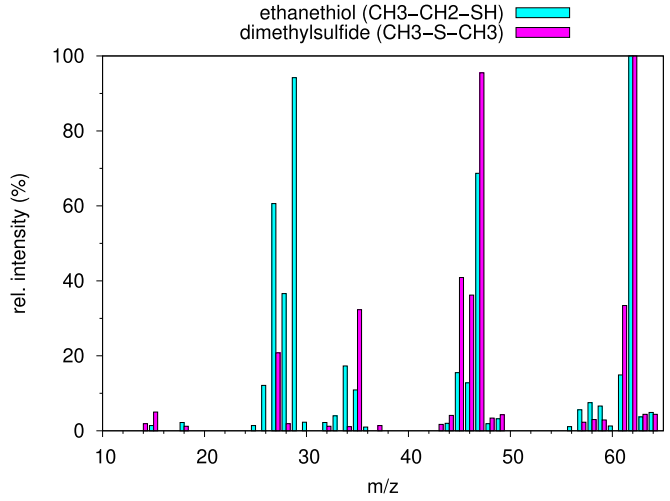

Figure 1. Juxtaposed NIST reference fragmentation patterns of the two structural isomers DMS and ethanethiol (S. E. Steins 2018). The relative intensity (rel. intensity; normalized to the highest signal in the spectrum) is plotted as a function of mass per charge (m/z).

charged species, parents, and fragments. If the gaseous analyte is a complex mixture, such as that from a cometary coma, the fragmentation patterns of all species that are simultaneously ionized in the instruments' ionization chamber overlap, and the sum of their fragmentation patterns is detected. As it is not possible to calibrate all volatile organic molecules on the DFMS laboratory twin instrument and the DMFS calibration facility is not equipped for handling corrosive or toxic species, like for instance DMS, we used reference fragmentation patterns from the National Institute of Standards and Technology (NIST) chemistry web-book EI-MS database (S. E. Steins 2018) for this work. Fragmentation patterns measured with DFMS are known to deviate little from those in the NIST database; see, e.g., M. Schuhmann et al. (2019a, 2019b). This deviation is mostly due to the different ionization energies—DFMS uses 45 eV electrons, while NIST standard spectra are usually measured using 70 eV electrons. The ionization cross section of DMS changes little between 45 and 70 eV (J. Kaur et al. 2015). By trend, lower ionization energies may slightly enhance the relative abundance of the parent with respect to the fragments. Also, differences in instrument geometries may play a role. Here, we do not account for those deviations. However, calibration experiments performed by M. Schuhmann et al. (2019a, 2019b) and in the framework of several PhD theses (U. M. Calmonte 2015; I. R. H. G. Schroeder 2020; M. Schuhmann 2020) archived together with the ROSINA data on ESA's Planetary Science Archive and NASA's Planetary Data System show that they are generally small, normally below 10% relative intensity. Figure 1 juxtaposes the NIST fragmentation patterns of DMS and its structural isomer ethanethiol, the topic of this work, normalized to the highest signal. The most intense signal in both fragmentation patterns is the M signal on $m/z = 62$. Both isomers also produce a relevant M-H signal on $m/z = 61$, which for DMS is more pronounced. The lower-mass fragments, however, are distinct: DMS favorably loses a methyl group, leading to a strong group of signals on $m/z = 45$–47, the M-CH_3 fragment being the one on $m/z = 47$. Ethanethiol may also lose a methyl group but more favorably loses the thiol function to produce a set of strong signals on $m/z = 27$–29. Below, we discuss which features are used to distinguish the two molecules based on ROSINA/DFMS mass spectra.

2.3. Data Reduction

Figure 2 shows the mass spectra registered around the nominal masses $m/z = 62$, where we expect the M of DMS (C_2H_6S = M), and $m/z = 61$, where, according to NIST (S. E. Steins 2018), we expect an abundant DMS fragment (C_2H_5S = M-H). Here, we describe the data reduction routine to extract the relative intensities from ROSINA/DFMS mass spectra.

In a first step, the absolute peak position and, consequently, the mass scale in the mass spectrum have to be defined via one known species-peak pair. Frequently observed continuation of homologous series in adjacent mass spectra (e.g., C_2H_5S and C_2H_6S in Figure 2) as well as regularly measured and abundant cometary species like H_2O, CO, CO_2, COS, or CS_2 are helpful to verify the mass scale. The mass scale around $m/z = 61$ and 62 is very well constrained by the strong signals of COS and its isotopologue $OC^{34}S$ on $m/z = 60$ and 62, respectively, as well as by the SO_2 and S_2 signal on $m/z = 64$. The pixel zero (p_0), i.e., the pixel of the commanded integer mass, shifts only little ($\approx$0.3 pixel) from one mass scan to the next.

Subsequently, the signal strengths must be extracted via peak fitting, using a Gaussian peak profile on a linear background; see, e.g., L. Le Roy et al. (2015). A good fit is usually achieved by combining an intense and narrow first Gaussian with a less intense and broader second Gaussian with fixed height and width ratios (J. De Keyser et al. 2019). Here, we used a double-Gaussian peak profile for signals with intensities above 10 a.u. and a single-Gaussian one for smaller signals where the second Gaussian disappears in the background. It can be seen from Figure 2 that signals from multiple species are usually present in one mass spectrum. Thanks to the high mass resolution of DFMS, it is often possible to distinguish species that have only small differences in the exact masses. The fitted peak position for the signal attributed to C_2H_6S is 62.0185 ± 0.0005 (the exact mass being at $m/z = 62.0190$), and for the signal attributed to C_2H_5S it is 61.0116 ± 0.0008 (the exact mass being at $m/z = 61.0112$). Hence, both peak positions lie within 1σ from the expected peak positions of C_2H_6S and C_2H_5S. The next closest possible species, C_5H_2 and C_5H, have a mass difference of 7σ and 4.5σ, respectively, which renders their contributions negligible. The fit error for the peak area is 3.6% for C_2H_6S and 8% for C_2H_5S. The reduced χ^2 for the overall fit is 0.998 for $m/z = 62$ and 0.992 for $m/z = 61$.

Sometimes, corrections for a drift in the signal strength during the time of the data collection are necessary as a change in cometary outgassing activity potentially distorts the observed fragmentation patterns. However, no such correction was implemented as the isotopic ratios of CO_2 and COS match the expectations (U. Calmonte et al. 2017; M. Hässig et al. 2017), which indicates stable coma conditions on the time-scales relevant for this investigation. Also, the water signal on $m/z = 18$, additionally scanned first and last in every mode to track density fluctuations, shows <3% variation. In addition, the instrument sensitivity changes as a function of mass and varies for the different species. We accounted for the mass-dependent sensitivity change according to the description, e.g., in L. Le Roy et al. (2015). As the species-dependent sensitivities are not known, it is not possible to derive the signal strength as number of ions per time, and we show it in

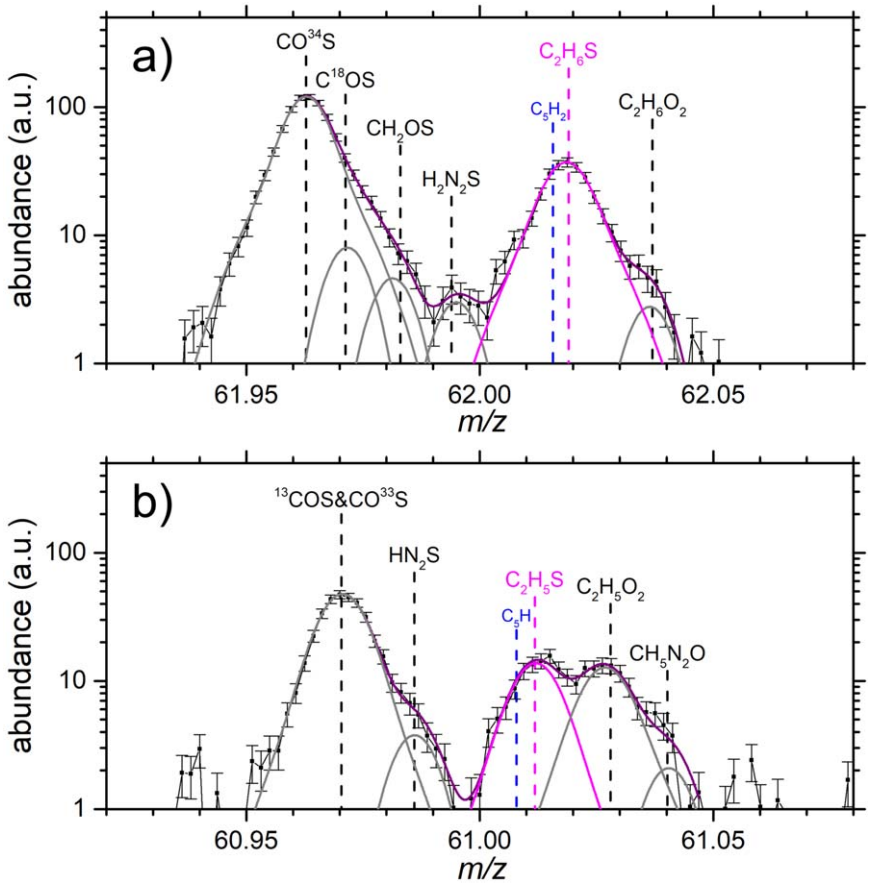

Figure 2. DFMS mass spectra collected on 2016 March 15 around m/z equal to 62 (a) and 61 (b). The measured intensities per pixel are plotted with black squares, in arbitrary units (a.u.), and with their statistical uncertainties. The peaks are fitted with Gaussian functions. We show the individual Gaussians in gray, highlighting those representing the relevant S-bearing species in magenta, and the overall fit in purple. The exact mass positions of the different chemical species are indicated by dashed lines. The standard deviation of the fitted peak position is $\approx 6 \times 10^{-4}$.

arbitrary units (a.u.). However, N_2 gas was used to calibrate the DFMS detector, and the established conversion factor was applied to allow a quantitative interpretation of the resulting numbers as N_2^+ ion equivalents. The estimated errors in the signal intensities of the C_nH_mS (n and m being the stoichiometric coefficients of C and H, respectively) species targeted in this work are ≈15%. This estimation for the overall errors includes (1) a statistical error (negligible for the signals under consideration except for the very low-abundance ones like C_2H_3S), (2) a fit error, and (3) an error related to different signal gains of the individual pixels. Errors related to the detector gain cancel out as all species were measured on the highest gain step. The nonnegligible statistical error for low-abundance species increases the respective overall error to be 20%. A 20% overall error was also estimated for CH_3S on $m/z = 47$. While the counting statistics are good for CH_3S, its exact mass is very close to $^{13}C^{16}O^{18}O$, an isotopologue of the abundant cometary volatile CO_2, and no distinction by fitting is possible. The observed signal was hence corrected by subtracting 1.2% of the signal of $^{12}C^{16}O^{18}O$ on $m/z = 46$ based on the carbon isotope ratio measured in CO_2 (M. Hässig et al. 2017). The latter is separable from CH_2S by fitting. The C_2H_4S signal on $m/z = 60$ has an even larger overall error of 50% as this species is fully in the slope of the large peak of the main COS isotopologue, which increases the fit's uncertainties considerably.

3. Results and Discussion

The fits presented in Figure 2 and discussed above allow unambiguous association of the observed signals to C_2H_6S and C_2H_5S, respectively, and show that the contribution of the pure hydrocarbon species (C_5H_2 and C_5H) are negligible. The corrected observed intensities (in a.u.) are now compared to the reference fragmentation patterns from NIST. Figure 3 shows the observed intensities of organosulfur species between $m/z = 45$ and 62 and how they compare to the expected intensities (S. E. Steins 2018) for the possible combinations of parent molecules. The most striking difference between the two isomers, DMS and ethanethiol, manifests itself with regard to the C_2H_5S signal at $m/z = 61$, corresponding to M-H of both candidates. While fragmentation of DMS explains the observed C_2H_5S signal within 1σ error margins (top panel), the expected ethanethiol fragment intensity is off from the observed signal by more than 3σ (bottom panel). The same findings result from the investigation of additional mass spectra collected on the same day (2016 March 15) at different times as well as 2 days later (2016 March 17). In the Appendix, Figure 4 plots the additional data and Table 1 lists the derived C_2H_5S/C_2H_6S ratios that are compatible, within error limits, with DMS but not with ethanethiol.

The observed C_2H_3S signal on $m/z = 59$, corresponding to approximately 8% of the C_2H_6S signal on $m/z = 62$, is only partially due to the M-3H fragment of DMS or ethanethiol, respectively. The unexplained intensity most likely indicates

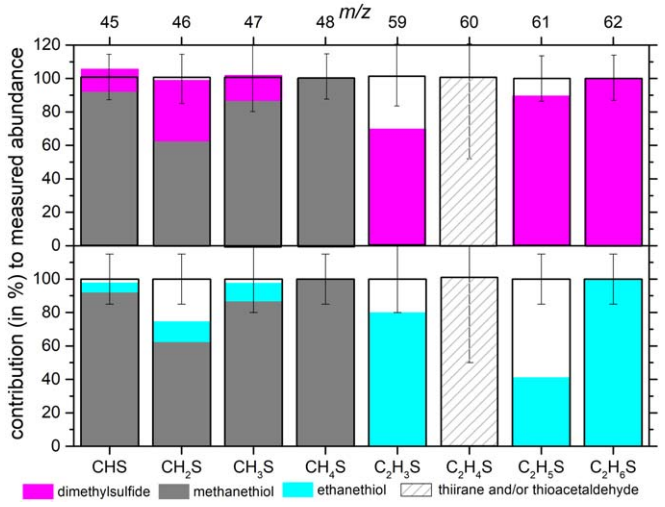

Figure 3. Measured vs. expected intensities for the two combinations methanethiol + DMS (top) and methanethiol + ethanethiol (bottom). Color coded are the individual contributions in percent of the observed intensity. Reference spectra have been taken from NIST (S. E. Steins 2018) and were scaled to C_2H_6S on $m/z = 62$ for both DMS and ethanethiol and to CH_4S on $m/z = 48$ for methanethiol as those species can be unambiguously assigned to the respective M. The hatched contribution to C_2H_4S on $m/z = 60$ can be assigned to thiirane and/or thioacetaldehyde (parent), fragments of which we do not indicate as no reference spectrum is available for thioacetaldehyde. Details are given in the main text.

the presence of an additional low-abundance parent with a molecular sum formula of C_2H_4S and a nominal mass of 60 Da that produces a C_2H_3S (M-H) fragment on $m/z = 59$. Unfortunately, the C_2H_4S signal is hidden below the flank of the strong COS signal and can only be retrieved from the data with an uncertainty as large as 50% (hatched bar in Figure 3). Attributing the C_2H_4S signal to either thiirane or thioacetaldehyde (or a mixture of both), the two structural isomers of C_2H_4S, likely explains the C_2H_3S intensity yet is unexplained by DMS or ethanethiol. While the thiirane fragmentation pattern from S. E. Steins (2018) is compatible with the residual intensities in Figure 3 (notably DMS residual intensities seem to fit better than those from ethanethiol), the fragmentation pattern of thioacetaldehyde is unknown. Similar to aldehydes, preferred loss of the aldehyde hydrogen atom is likely for thioacetaldehyde, which might lead to strong M and M-H signals too. It has to be stated clearly that, due to the large error margins of the signals and the missing fragmentation information for thioacetaldehyde, no conclusions can be drawn from the C_2H_3S signal as to which of the two C_2H_6S isomers produces a better match. Alternatively, heavier organosulfur species might yield C_2H_3S as a fragment; see further discussion of heavier organosulfur species below.

Last but not least, the observed signals on $m/z = 45$–47 also favor the presence of DMS over that of ethanethiol. While these signals are mostly attributed to methanethiol (CH_4S) and its fragments (gray bars in Figure 3) and contributions of the C_2H_6S isomers are minor, the CH_2S fragment on $m/z = 46$ leaves sufficient residual intensity after subtraction of the methanethiol contribution to be distinctive: again, the DMS contribution matches the missing intensity almost perfectly ($<1\sigma$ difference), while the ethanethiol contribution does not (approximately 2σ difference).

Based on Figure 3 as well as Figure 4 and Table 1 in the Appendix, DMS consistently reproduces the observed intensities together with methanethiol much better than ethanethiol. However, fragmenting heavier organosulfur species could contribute to the signals between $m/z = 45$ and 61, especially to $m/z = 61$ (C_2H_5S) and 46 (CH_2S), and explain the intensity that is left unexplained in Figure 3 (bottom). We ruled out this possibility based on the following line of reasoning:

1. The signal of fully saturated C_2H_6S on $m/z = 62$ can only indicate DMS or ethanethiol or a combination of both, but it cannot be a charge-retaining fragment of a heavier organosulfur as such fragments would be unsaturated. Approximately 40% of the observed intensity on C_2H_5S on $m/z = 61$ cannot be explained if all the C_2H_6S signal on $m/z = 62$ is associated to ethanethiol. If there are no heavier organosulfur parent species whose fragments could explain this residual intensity, then DMS is the only explanation.
2. Therefore, we searched the ROSINA/DFMS data for observed signals of parent species that theoretically yield C_2H_5S on $m/z = 61$. Candidate molecules must contain at least two C atoms, five H atoms, and one S atom. S-bearing species with molecular masses larger than 61 Da observed on 2016 March 15 are S_2 and SO_2, both registered on $m/z = 64$, as well as CS_2 on $m/z = 76$, and their minor isotopologues. Those species are abundant and well-studied coma species (L. Le Roy et al. 2015; U. Calmonte et al. 2016). However, they cannot produce the C_2H_5S fragment signal on $m/z = 61$ and therefore are not relevant. Up to $m/z = 100$, corresponding to the upper end of the mass range scanned on that day, no species that could contribute to the C_2H_5S fragment were observed. Apart from a few pure hydrocarbon species (C_mH_n), only krypton isotopes have been detected.
3. The picture is different when the comet was close to its perihelion at the beginning of 2015 August. N. Hänni et al. (2022) presented and discussed a data set collected on 2015 August 3, when the mass range was scanned up to $m/z = 140$ and the comet's coma was dusty. They reported the presence of a series of C_mH_nS-bearing species, which shows that DFMS is indeed able to identify these species—if they were present. The same authors derived upper limits in cases where distinction of the pure hydrocarbon and the S-bearing species with the same nominal mass was not possible as the exact masses are inseparable even at the mass resolution of DFMS. Intensities at the positions of the following C_2H_5S-bearing species have been observed: C_3H_5S, C_3H_6S, C_3H_8S, C_4H_5S, C_4H_6S, C_6H_8S, C_3H_5OS, C_3H_6OS, C_3H_7OS, C_4H_8OS, and $C_2H_6S_2$. We carefully checked if those species and their potential fragments, which are mostly $m/z = 57$, 64, 74, 76, 84, and 94 according to S. E. Steins (2018), are present also on 2016 March 15. However, the observed intensities are compatible with relevant and securely identified pure hydrocarbon species such as benzene. No sign of C_2H_5S-bearing species could be found.
4. The exact mass scale and isotopic relative abundances also exclude contributions of C_2H_6S isotopologues. They are well below the uncertainty of the measurements.

Having ruled out contributions of heavier organosulfur species, we find DMS compatible (deviations between expected and observed intensities $<1\sigma$) and ethanethiol much

less compatible (deviations between expected and observed intensities 2–4σ) with ROSINA/DFMS data from 2016 March 15 and 17. Neither DMS nor possible precursors such as DMSP or other C–S-bearing molecules have been detected in the spacecraft background (B. Schläppi et al. 2010), and also, reactions at the hot filament of the DFMS' ionization chamber are highly unlikely. Industrially, DMS is produced from the reaction of methanol and hydrogen disulfide over a hot aluminum oxide catalyst (K.-M. Roy 2000). Both these molecules are common in comets, including comet 67P, where their abundance usually is on the order of 1% relative to water (M. Rubin et al. 2019). Nevertheless, the ionization chamber's open design, which does not allow pressure buildup, as well as the shielding of the hot filament impede chemical reactions. The ion source itself remained below 25°C during the whole mission. We therefore argue that the observed DMS must be of cometary origin. Various lines of evidence, collected in N. Hänni et al. (2022), indicate a formation of volatile cometary organic molecules in the early solar system history rather than on the comet itself.

In order to estimate the abundance of DMS in comet 67P, we sum over all signals associated to DMS in the data set collected on 2016 March 15 between 03:30 and 04:14 UTC and give the result relative to methanol (CH_3OH). Methanol, a representative of complex organic molecules such as DMS itself, is not only common in comets but also in the interstellar medium (ISM); see, e.g., D. Bockelée-Morvan et al. (2000) or M. N. Drozdovskaya et al. (2019). From the analyzed spectra (Figures 2 and 3), we derive a relative abundance DMS/methanol $= (0.13 \pm 0.04)\%$ and methanethiol/methanol $= (0.9 \pm 0.27)\%$. The relatively large estimated error accounts for the circumstance that that neither the ionization cross sections nor the detector sensitivities of those molecules are known. Detailed information on the estimation of the error margins of abundances relative to methanol is in N. Hänni et al. (2023).

Notably, abundances of specific molecules in comet 67P may expose pronounced time variability. A time series for selected species has been published by M. Läuter et al. (2020). This time variability means that the relative abundance values reported for DMS in this work represent a snapshot. In Appendix A.1, we delve into the time variability by comparing the data shown in Figures 2 and 3 to other data sets collected around the time of 67P's outbound equinox in 2016 March; in 2014 October (U. Calmonte et al. 2016), while the spacecraft was orbiting the comet at a constant cometocentric distance of 10 km for roughly two weeks; and during its perihelion passage in early 2015 August (N. Hänni et al. 2022). Due to contamination of the data by heavy organosulfur species, full deconvolution is only possible for the 2016 March data. Although the signals are varying slightly in intensity, as can be seen in Figure 4 in the Appendix, the deduced C_2H_5S/C_2H_6S abundance ratios collected in Table 1 in the Appendix remain stable within error margins. Three out of four ratios are compatible with DMS as parent molecule within 1σ, while all four are off from the expectation value for ethanethiol by more than 3σ. Furthermore, the C_2H_6S/CH_4O abundance ratios were tabulated for the said data sets and demonstrate stability under similar conditions (2016 March and 2014 October). While demanding more detailed correlation studies similar to the work done by M. Rubin et al. (2023), this might hint at a shared origin of DMS and methanol not only in the comet but maybe even in the formational history. Additional pieces of the puzzle may be obtained from comparing the chemical complexity associated with cometary bulk ices (M. Rubin et al. 2019; M. Schuhmann et al. 2019a, 2019b) to that associated to dust (K. Altwegg et al. 2020, 2022; N. Hänni et al. 2022, 2023).

4. Conclusions

On Earth, DMS is a degradation product of DMSP, a sulfur-bearing compound produced by eukaryotic marine phytoplankton and a few higher plants (M. O. Andreae & H. Raemdonck 1983; C. B. Pilcher 2003). It has been proposed (S. Seager et al. 2013) and employed (N. Madhusudhan et al. 2021, 2023) as a unique biosignature in the search for biological activity on exoplanets. A thorough reanalysis of the high-resolution mass spectra collected by ROSINA/DFMS at comet 67P around the time of its outbound equinox, when U. Calmonte et al. (2016) have previously reported a C_2H_6S signal, provides strong evidence for the presence of DMS in cometary matter. This is the first evidence of a nonanthropogenic abiotic formation pathway. However, whether or not the existence of cometary, abiotic DMS is relevant to exoplanetary atmospheres and hence has implications for the use of DMS as a biosignature remains to be investigated in future work. E. C. Fayolle et al. (2017) have hypothesized for the case of chloromethane (CH_3Cl), which is considered a biosignature attributed to oceanic bacteria on Earth (S. Seager et al. 2016) and has been detected in comet 67P, that exocomets impacting young exoplanetary surfaces may have delivered considerable amounts of material, including $6 * 10^5$ kg yr^{-1} of CH_3Cl under peak influx conditions (R. Brasser et al. 2016). It is a topic of debate, though, if such a scenario is generally realistic or applicable to DMS and potentially other cometary species. Independent of DMS being employed as a biosignature, we hope the detection of this molecule in pristine cometary matter encourages studies of abiotic formational pathways, for instance, for dark molecular cloud conditions or protostellar environments. Given its respectable abundance relative to methanol derived from this work, DMS may be a promising candidate for ISM molecular searches (spectroscopic reference data are available from A. Jabri et al. 2016 and V. Ilyushin et al. 2020). Laboratory work by A. Mahjoub et al. (2017) with astrochemical ice analogs containing hydrogen sulfide and methanol showed a signal on $m/z = 62$ upon electron irradiation followed by temperature-programmed desorption. However, the presented identification of DMS by these authors misses acknowledging the ambiguities created by unit mass resolution EI-MS and simultaneous sublimation of various sulfur-bearing molecules. Our results strongly motivate further investigation of the ISM sulfur ice chemistry as started by A. Mahjoub et al. (2017), instead focusing on the combination of small reduced sulfur and carbon carriers such as hydrogen sulfide and methane.

Acknowledgments

We gratefully acknowledge the work of the many engineers, technicians, and scientists involved in the Rosetta mission and in the planning, construction, and operation of the ROSINA instrument. Without their contributions, ROSINA would not have produced such outstanding data and scientific results. Rosetta is an ESA mission with contributions from its member states and NASA. Work at the University of Bern was funded by the Canton of Bern and the Swiss National Science

Foundation (200020_207312). M.C. acknowledges support from NASA grants 80NSSC18K1280 and 80NSSC20K0651. J.D.K. acknowledges support from the Belgian Science Policy Office through PRODEX/ROSINA PEA 4000090020 and 4000107705. N.F.W.L. acknowledges support from the Swiss National Science Foundation (SNSF) Ambizione grant 193453. S.F.W. acknowledges support of the SNSF Eccellenza Professorial Fellowship PCEFP2_181150. We are grateful to Daniel Kitzmann for the enlightening discussions on the JWST observations of K2-18b.

Appendix
Appendix Information

A.1. Time Variability of the Targeted Signals

In order to investigate the time variability of the targeted S-bearing species, we have compared several $m/z = 62$ and $m/z = 61$ ROSINA/DFMS mass spectra mostly from 2016 mid-March; see Figure 4 and Table 1. In 2016 March, comet 67P passed its outbound equinox, with the spacecraft at a heliocentric distance of 2.58 au and at a cometocentric distance of approximately 13.5 km. Due to the rotation of the comet and the orbit of the spacecraft, the observable longitudes and latitudes were constantly changing on a short timescale, although DFMS has a large field of view of 20°. In addition to the short-term variability, observed as a result of said changes in observational geometries or in cometary activity, there are other factors having an impact in the long term. As the comet moved around the Sun and passed its dust and gas outflow activity maximum shortly after reaching perihelion in 2015 August, the Rosetta orbiter had to constantly readjust its relative position to the comet's surface for safety reasons. Sometimes, the distance also was changed for scientific reasons. For instance, shortly after the 2016 mid-March data were collected, the spacecraft retracted from the comet in favor of plasma studies to much greater cometocentric distances. As the local densities vary with $1/r^2$, where r is the cometocentric distance, relatively weak signals, <1% relative to water, are difficult to observe. For this reason, DMS was mainly observed when the spacecraft was close to the comet's surface at the beginning of the mission or around the analyzed equinox period. Its characteristic signal, i.e., C_2H_6S on $m/z = 62$, was just above detection limit when the comet was very active around perihelion, even though the spacecraft was at a relatively large cometocentric distance.

Table 1 summarizes the spacecraft's relative position together with the C_2H_5S/C_2H_6S and the C_2H_6S/CH_4O abundance ratios for the four spectra shown in Figure 4 plus two additional ones. For the latter two, from 2014 October 10 (U. Calmonte et al. 2017) and 2015 August 3 (N. Hänni et al. 2022), no full analysis can be done as, in both cases, heavier C_nH_mS species and potentially even C_5H are contaminating the C_2H_5S signal. The derived C_2H_5S/C_2H_6S ratios thus have a large uncertainties. From the listed abundance ratios we can conclude two things: First, three out of four C_2H_5S/C_2H_6S abundance ratios are compatible with DMS within 1σ, while for ethanethiol all are off by more than 3σ. Note that for DMS, the expected C_2H_5S/C_2H_6S ratio is 33%, while for ethanethiol it is 15% (S. E. Steins 2018). Second, the C_2H_6S/CH_4O abundance ratios, where CH_4O corresponds to the methanol M, are surprisingly constant too, except for the one in 2015 August, when there was a lot of sublimation also from dust and the cometary activity was highly variable. In 2014 October and 2016 March, however, the comet was at a comparable heliocentric distance of around 3 au, and the activity was more stable and rather comparable. The respective C_2H_6S/CH_4O abundance ratios are identical within 1σ error margins. This is an indication for DMS and methanol to sublimate from the same layer in the cometary nucleus and possibly even hints at a common origin. However, more detailed correlation studies are needed to support this hypothesis.

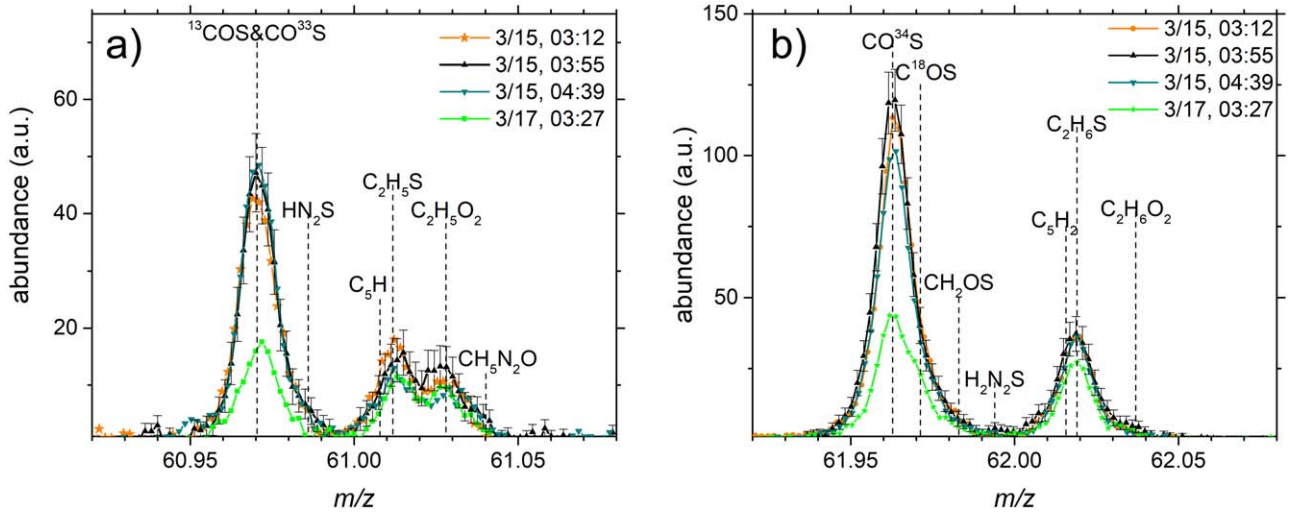

Figure 4. Time variability of DFMS mass spectra collected around 67P's outbound equinox and for the set masses $m/z = 61$ (a) and $m/z = 62$ (b). The measured intensities per pixel are plotted with line points and in arbitrary units (a.u.). To improve the visibility, statistical uncertainties are indicated as error bars for the March 15 03:55 UTC spectrum only.

Table 1
Spacecraft Relative Position (Longitude and Latitude) and C_2H_5S/C_2H_6S and C_2H_6S/CH_4O Abundance Ratios for the Four Spectra Shown in Figure 4 plus Two Additional Spectra from 2014 October 10 (U. Calmonte et al. 2016) and 2015 August 3 (N. Hänni et al. 2022)

Time (UTC)	Longitude (deg)	Latitude (deg)	C_2H_5S/C_2H_6S (%)	C_2H_6S/CH_4O (%)
2016 Mar 15, 03:12	29.08	−14.63	43 ± 6	0.13 ± 0.04
2016 Mar 15, 03:55	7.37	−17.10	31 ± 6	0.13 ± 0.04
2016 Mar 15, 04:40	−14.40	−19.59	36 ± 6	0.14 ± 0.04
2016 Mar 17, 03:27	−140.18	21.42	40 ± 7	0.11 ± 0.04
2014 Oct 10, 17:17	−13.45	6.59	100 ± 20	0.12 ± 0.04
2015 Aug 3, 16:48	−31.09	−13.78	95 ± 30	0.26 ± 0.06

ORCID iDs

Nora Hänni https://orcid.org/0000-0002-8253-6436
Kathrin Altwegg https://orcid.org/0000-0002-3946-2320
Michael Combi https://orcid.org/0000-0002-9805-0078
Johan De Keyser https://orcid.org/0000-0003-4805-5695
Niels F. W. Ligterink https://orcid.org/0000-0002-8385-9149
Martin Rubin https://orcid.org/0000-0001-6549-3318
Susanne F. Wampfler https://orcid.org/0000-0002-3151-7657

References

Altwegg, K., Balsiger, H., & Fuselier, S. A. 2019, ARA&A, 57, 113
Altwegg, K., Balsiger, H., Hänni, N., et al. 2020, NatAs, 4, 533
Altwegg, K., Combi, M., Fuselier, S. A., et al. 2022, MNRAS, 516, 3900
Andreae, M. O., & Raemdonck, H. 1983, Sci, 221, 744
Balsiger, H., Altwegg, K., Bochsler, P., et al. 2007, SSRv, 128, 745
Bardyn, A., Baklouti, D., Cottin, H., et al. 2017, MNRAS, 469, S712
Bieler, A., Altwegg, K., Balsiger, H., et al. 2015, Natur, 526, 678
Bockelée-Morvan, D., Lis, D. C., Wink, J. E., et al. 2000, A&A, 353, 1101
Bouquet, A., Mousis, O., Waite, J. H., & Picaud, S. 2015, GeoRL, 42, 1334
Brasser, R., Mojzsis, S. J., Werner, S. C., Matsumura, S., & Ida, S. 2016, E&PSL, 455, 85
Calmonte, U., Altwegg, K., Balsiger, H., et al. 2016, MNRAS, 462, S253
Calmonte, U., Altwegg, K., Balsiger, H., et al. 2017, MNRAS, 469, S787
Calmonte, U. M. 2015, PhD thesis, Univ. of Bern
Catling, D. C., Krissansen-Totton, J., Kiang, N. Y., et al. 2018, AsBio, 18, 709
De Keyser, J., Altwegg, K., Gibbons, A., et al. 2019, IJMSp, 446, 116232
Domagal-Goldman, S. D., Meadows, V. S., Claire, M. W., & Kasting, J. F. 2011, AsBio, 11, 419
Drozdovskaya, M. N., van Dishoeck, E. F., Rubin, M., Jørgensen, J. K., & Altwegg, K. 2019, MNRAS, 490, 50
Fayolle, E. C., Öberg, K. I., Jørgensen, J. K., et al. 2017, NatAs, 1, 703
Glein, C. R. 2024, ApJL, 964, L19
Hänni, N., Altwegg, K., Baklouti, D., et al. 2023, A&A, 678, A22
Hänni, N., Altwegg, K., Combi, M., et al. 2022, NatCo, 13, 3639
Hänni, N., Gasc, S., Etter, A., et al. 2019, JPCA, 123, 5805
Hässig, M., Altwegg, K., Balsiger, H., et al. 2017, A&A, 605, A50
Horita, J., & Berndt, M. E. 1999, Sci, 285, 1055
Ilyushin, V., Armieieva, I., Dorovskaya, O., et al. 2020, JMoSt, 1200, 127114
Jabri, A., Van, V., Nguyen, H. V. L., et al. 2016, A&A, 589, A127
Kaur, J., Singh, S., & Antony, B. 2015, MolPh, 113, 3883
Läuter, M., Kramer, T., Rubin, M., & Altwegg, K. 2020, MNRAS, 498, 3995
Le Roy, L., Altwegg, K., Balsiger, H., et al. 2015, A&A, 583, A1
López-Gallifa, Á., Rivilla, V. M., Beltrán, M. T., et al. 2024, MNRAS, 529, 3244
Madhusudhan, N., Piette, A. A. A., & Constantinou, S. 2021, ApJ, 918, 1
Madhusudhan, N., Sarkar, S., Constantinou, S., et al. 2023, ApJL, 956, L13
Mahjoub, A., Altwegg, K., Poston, M. J., et al. 2023, SciA, 9, eadh0394
Mahjoub, A., Poston, M. J., Blacksberg, J., et al. 2017, ApJ, 846, 148
Pilcher, C. B. 2003, AsBio, 3, 471
Poch, O., Istiqomah, I., Quirico, E., et al. 2020, Sci, 367, aaw7462
Raulin, F., & Toupance, G. 1975, OrLi, 6, 91
Rigby, F. E., & Madhusudhan, N. 2024, MNRAS, 529, 409
Roy, K.-M. 2000, Thiols and Organic Sulfides (New York: Wiley),
Rubin, M., Altwegg, K., Balsiger, H., et al. 2019, MNRAS, 489, 594
Rubin, M., Altwegg, K., Berthelier, J.-J., et al. 2023, MNRAS, 526, 4209
Sagan, C., Thompson, W. R., Carlson, R., Gurnett, D., & Hord, C. 1993, Natur, 365, 715
Sandford, S. A. 2008, ARAC, 1, 549
Schläppi, B., Altwegg, K., Balsiger, H., et al. 2010, JGRA, 115, A12313
Schroeder, I. R. H. G. 2020, PhD thesis, Univ. of Bern
Schuhmann, M. 2020, PhD thesis, Univ. of Bern
Schuhmann, M., Altwegg, K., Balsiger, H., et al. 2019a, ESC, 3, 1854
Schuhmann, M., Altwegg, K., Balsiger, H., et al. 2019b, A&A, 630, A31
Schwieterman, E. W., Kiang, N. Y., Parenteau, M. N., et al. 2018, AsBio, 18, 663
Seager, S., Bains, W., & Hu, R. 2013, ApJ, 777, 95
Seager, S., Bains, W., & Petkowski, J. J. 2016, AsBio, 16, 465
Shorttle, O., Jordan, S., Nicholls, H., Lichtenberg, T., & Bower, D. J. 2024, ApJL, 962, L8
Steins, S. E. 2018, Chemistry WebBook (Gaithersburg, MD: NIST) NIST Standard Reference Database Number 69
Taubner, R.-S., Pappenreiter, P., Zwicker, J., et al. 2018, NatCo, 9, 748
Waite, J. H., Glein, C. R., Perryman, R. S., et al. 2017, Sci, 356, 155
Wogan, N. F., Batalha, N. E., Zahnle, K. J., et al. 2024, ApJL, 963, L7